Physica E 44 (2012) 944–948

Contents lists available at SciVerse ScienceDirect

Physica E

journal homepage: www.elsevier.com/locate/physe

Buckling of peapods, fullerenes and nanotubes

Nicola M. Pugno [a,*], James A. Elliott [b]

[a] Laboratory of Bio-Inspired Nanomechanics "Giuseppe Maria Pugno", Department of Structural Engineering and Geotechnics, Politecnico di Torino, Corso Duca degli Abruzzi 24, 10129, Torino, Italy
[b] Department of Materials Science and Metallurgy, University of Cambridge, Pembroke Street, Cambridge CB2 3QZ, UK

ARTICLE INFO

Article history:
Received 22 July 2010
Received in revised form
1 December 2011
Accepted 30 December 2011
Available online 6 January 2012

ABSTRACT

In this paper, the buckling under an applied external pressure and the self-buckling of nanostructures, such as peapods, nanotubes and fullerenes, is numerically treated with Molecular Dynamics simulations and compared with theoretical calculations. The self-buckling is due to the interaction among the nanostructures caused by the surface energy; it is peculiar to the nanoscale and does not have a macroscopiic counterpart. Atomistic simulations confirm that the influence on a single nanostructure from the surrounding nanostructures in a crystal, is nearly identical to that of a liquid with surface tension equal to the surface energy of the solid.

1. Introduction

Nanoscopic graphite filaments caught the attention of materials scientists due to their outstanding mechanical properties, which are closely related to those of graphite in the basal plane (see, for example, [1]), even before the identification of carbon nanotubes (CNTs) as graphene layers rolled into cylinders with hemispherical fullerene caps [2]. Experimental [3–5] and theoretical works [6,7] indicate that the axial stiffness and strength of CNTs are of the order of 1 TPa and 50 GPa, respectively, both in agreement with those for in-plane graphite [8] and graphene [9]. The interaction between walls in CNTs and the self-interaction of CNTs in bundles, mostly governed by van der Waals forces, is also similar to the interaction between graphene layers in graphite and results in a low shear strength between adjacent graphene layers that facilitates CNTs sliding [10]. The assembly of CNTs into a macroscopic long bundle composed of shorter fibres, a constraint still imposed by the current technology, is thus challenging due to the aforementioned weak shear interactions. The common orientation of the nanotubes along the bundle axis is a strategy consistent with the basic principles for making high performance fibres, the properties of which are derived from extended molecules oriented along their main axis and parallel to the fibre [11]. Indeed, CNT fibres with tensile properties in the high-performance range, e.g. that of aramid but still far from that of an individual CNT, are currently produced by various nanotechnology approaches.

A key factor for increasing the bundle strength is the self-buckling of the nanotubes [12]. The elastic buckling under applied mechanical pressure, and even in the absence of pressure, i.e. the self-buckling of nanotubes in a bundle, was investigated by atomistic simulations in [13]. These authors have performed Molecular Dynamics (MD) simulations to confirm that single-wall carbon nanotubes (SWCNTs) undergo a discontinuous collapse transition under hydrostatic pressure. They also predicted a critical diameter for the self-collapse of SWCNTs, at standard temperature and pressure, lying between 4.2 and 6.9 nm with the simple generic force field used. In addition, there was good agreement between their simulations, calibrated with X-ray compression data for graphite, and the experimentally observed transition pressures for laser-grown nanotubes. This level of agreement raised confidence that the simple and computationally inexpensive force field used [13] can be suitable for examining the nanomechanics of nanotubes.

Moreover, the self-buckling of nanotubes in a bundle has been experimentally observed [14]. These authors have introduced a method for the direct spinning of pure carbon nanotube fibres from an aerogel formed during chemical vapour deposition. The continuous withdrawal of product from the gas phase as a fibre imparts high commercial potential to the process, including the possibility of in-line post-spin treatments for further product optimisation. Also, these authors [14] have shown that the mechanical properties of the fibres are directly related to the type of nanotubes present (i.e., multiwall or single wall, diameters, etc.), which in turn, can be, at least ideally, controlled by the careful adjustment of process parameters. In particular, they obtained high performance fibres from dog-bone, i.e. self-collapsed, carbon nanotubes.

Only very recently, a full theoretical explanation of the self-buckling has been given, including its beneficial implication on the overall mechanical strength [12] in the case of sliding failure. Roughly, the self-collapse enlarges the interface surface area between the nanotubes and thus also the strength of the junctions between nanotubes and finally the overall fracture strength of the

* Corresponding author. Tel.: +39 011 090 4902; fax: +39 011 090 4899.
E-mail address: nicola.pugno@polito.it (N.M. Pugno).

1386-9477/$ - see front matter © 2012 Elsevier B.V. All rights reserved.
doi:10.1016/j.physe.2011.12.024

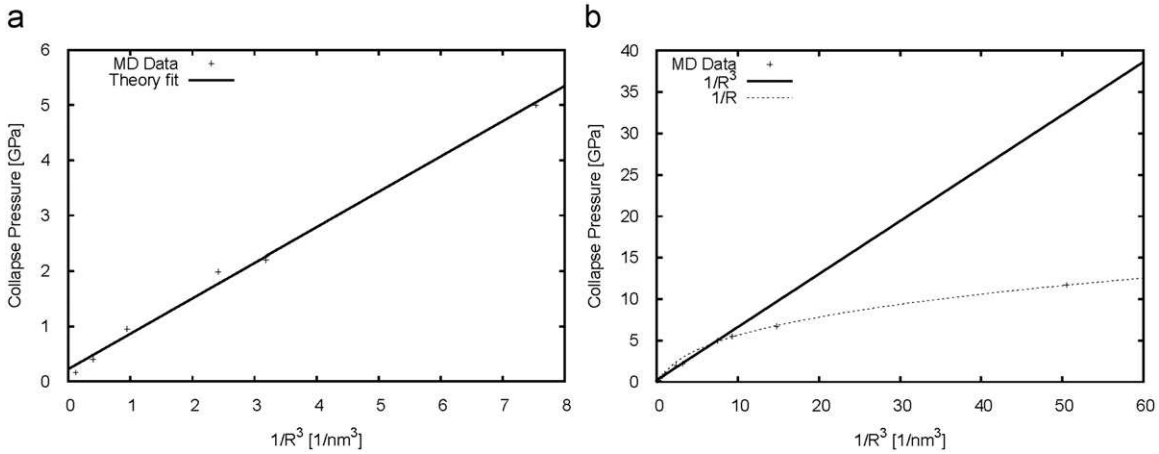

Fig. 1. Critical collapse pressure for SWCNTs in a bundle, with data points calculated according to MD simulations [13], fitted by: (a) relationship for critical pressure (Eq. (1)), expressed as $p_C+\gamma/R$ vs. $1/R^3$ and shown by solid line with gradient 3D, and (b) extrapolation of fit to tubes with smaller diameter, with alternative fit of $p_C+const$ vs. $1/R$ shown by dotted line.

Table 1
Collapse pressure of SWCNTs and DWCNTs in a bundle: comparison of MD simulations to theory. (–) indicates tube diameter too small to be fitted by Eq. (1).

Nanotube	Diameter [nm]	Collapse pressure [GPa] (MD)	Collapse pressure [GPa] (Eq. (1))
(7,0)	0.54	11.70	–
(6,6)	0.82	6.70	–
(7,7)	0.95	5.50	–
(13,0)	1.02	5.00	5.05
(10,10)	1.36	2.20	2.27
(11,11)	1.49	1.91	1.76
(13,9)	1.50	2.03	1.74
(19,0)	1.49	1.99	1.76
(16,5)	1.49	1.98	1.76
(15,15)	2.04	0.95	0.83
(20,20)	2.72	0.40	0.48
(30,30)	4.08	0.16	0.30
{(15,15),(10,10)}	2.04/1.36	3.45	2.64
{(10,10),(5,5)}	1.36/0.68	9.47	8.37
{(11,11),(7,7)}	1.49/0.95	6.80–7.20	6.42
{(15,15),(7,7)}	2.04/0.95	1.00–3.00	2.64

bundle, in case of sliding failure. For the prediction of the complimentary intrinsic fracture see [15–22].

The present paper is focused on the buckling of peapods, nanotubes and fullerenes and compares new ad hoc Molecular Dynamics simulations with analytical results calculated according to the approach presented in [12]. In particular, Figs. 1, 3, 4, 6 and Table 1 show the main new results of the present paper.

2. Theory and molecular dynamic simulations

We treat the crystal as a liquid-like material with surface tension $\gamma_t=\gamma$, as imposed by the energy equivalence (the surface tension has the thermodynamic significance of work spent to create the unit surface, as the surface energy), thus deducing a pressure γ/R acting on a single nanotube of radius R within a bundle, as evinced by the Laplace's equation [12]. In other words, considering a cylindrical cavity/nanotube of size R under a pressure p in a liquid/nanotube bundle having surface tension/energy γ, the free energy (per unit length) of the system can be written as $E=-p(\pi R^2)+\gamma(2\pi R)+const$ and has to be minimal at the equilibrium; thus posing $dE=0$, we find $p=\gamma/R$. Note that for a crystal composed by fullerenes of radius R, the pressure $p=2\gamma/R$ on a fullerene could be deduced from $E=-p((4/3)\pi R^3)+\gamma(4\pi R^2)+const$ posing $dE=0$, again in agreement with the prediction of the Laplace's equation. Mixed systems, such as peapods, are also considered in this paper.

2.1. Nanotubes

The critical pressure p_C can be accordingly derived as [12]:

$$p_C=\frac{3N^\alpha D}{R^3}-\frac{\gamma}{R} \tag{1}$$

where N is the number of walls and $1\le\alpha\le 3$: assuming perfect bonding between the walls would correspond to $\alpha=3$, whereas for independent walls $\alpha=1$, D is the bending stiffness of graphene; however, note that in the equations it appears always as the group $N^\alpha D$, that is the total bending stiffness.

The first term in Eq. (1) is that governing the buckling of a perfectly elastic cylindrical long thin shell (of bending stiffness $N^\alpha D$), whereas the second term is the pressure imposed by the surrounding nanotubes, significant only at the nanoscale.

Treating the MD simulations results for single-wall carbon nanotubes (SWCNTs) [13], excluding the three smallest nanotubes for which the finite wall thickness becomes significant, a good agreement with Eq. (1) is observed, with plausible fitted values of $D_{fit}\approx 0.21$ nN nm and $\gamma_{fit}\approx 0.23$ N m^{-1}, as shown in Fig. 1(a). However, when data from the three smallest nanotubes were also considered, as shown in Fig. 1(b), a linear fit of the form $p_C\propto 1/R$ is more suitable, as found originally by Elliott et al. [13]. Furthermore, a new additional comparison between theory and MD simulations for single and double wall carbon nanotubes (DWCNTs) is reported in Table 1, showing a good agreement.

From Eq. (1) we derive the following condition for the self-collapse, i.e. collapse under zero pressure, of a nanotube in a bundle [12]:

$$R\ge R_C^{(N)}=\sqrt{\frac{3N^\alpha D}{\gamma}}=\sqrt{6}R_0^{(N)}. \tag{2}$$

Taking $D=0.1$ 1 nN nm and $\gamma=0.18$ N/m we find $2R_C^{(1)}\approx 2.7$ nm. Considering an intermediate coupling between the walls with $\alpha\approx 2$, the critical diameters for double and triple walled nanotubes are $2R_C^{(2)}\approx 5.4$ nm and $2R_C^{(3)}\approx 8.1$ nm. Note that for self-similar structures ($t/R=const$) the minimum thickness Nt ($D\propto t^3$) required for the self-buckling is very small, thus the self-collapse is peculiar to the nanoscale and does not have a macroscopic counterpart.

In [14], 17 experimental observations on the self-collapse of nanotubes in a bundle have been reported, see Fig. 2 and related Table 2. A number of 5 SWCNTs with diameters in the range 4.6–5.7 nm were all observed as collapsed; moreover, while the 3 doubly walled carbon nanotubes observed with internal diameters in the range 4.2–4.7 nm (the effective diameters are larger by a factor of $\sim$0.34/2 nm) had not collapsed, the observed 8 double-wall nanotubes with internal diameters in the range 6.2–8.4 nm had collapsed. Finally, a triple-wall nanotube of 14 nm internal diameter (the effective diameter is $\sim$14.34 nm) was also observed as collapsed. All 17 observations are in agreement with our theoretical predictions of Eq. (2), supporting our conjecture of liquid-like nanotube bundles [12].

2.2. Fullerenes

Similarly, the critical pressure of fullerenes in a fullerite crystal is [12]:

$$p_C = \frac{2}{\sqrt{3(1-\nu^2)}}\frac{N^\alpha E t^2}{R^2} - \frac{2\gamma}{R} \tag{3}$$

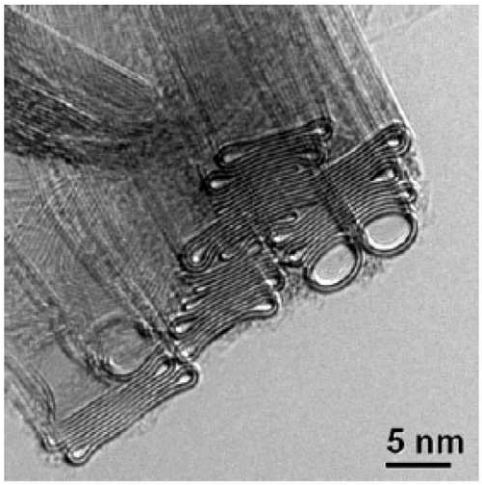

Fig. 2. Self-collapsed nanotubes in a bundle [14].

Table 2
Self-collapse of nanotubes in a bundle: theory [12] and MD simulations [13] exactly fit the experimental observations [14].

Nanotube number	Number N of walls	Diameter of the internal wall [nm]	Collapsed (Y/N) theo., MD and exp.
1	1	4.6	Y
2	1	4.7	Y
3	1	4.8	Y
4	1	5.2	Y
5	1	5.7	Y
6	2	4.2	N
7	2	4.6	N
8	2	4.7	N
9	2	6.2	Y
10	2	6.5	Y
11	2	6.8	Y
12	2	6.8	Y
13	2	7.9	Y
14	2	8.3	Y
15	2	8.3	Y
16	2	8.4	Y
17	3	14.0	Y

where $1 \le \alpha \le 2$ describes the interaction between the walls, E is the Young modulus and t is the monolayer thickness ($\sim$0.34 nm); the first term is that posed by elasticity (that considers $\alpha=2$; see for instance [12]), whereas the second one models the fullerene interaction, as previously discussed.

Note that the factor $(t/R)^2$ for fullerenes, appearing instead of $(t/R)^3$ for nanotubes, shows that the critical pressure for fullerenes is much higher than that for nanotubes, at least for $t/R \ll 1$.

From Eq. (3) we derive the following condition for the self-buckling [12]:

$$R_C^{(N)} = \frac{1}{\sqrt{3(1-\nu^2)}}\frac{N^\alpha E t^2}{\gamma}. \tag{4}$$

Note that for $\nu=0$, $N=1$, $E=1$ TPa, $t=0.34$ nm, $\gamma=0.2$ N/m, we find $R_C^{(1)} \approx 0.33$ μm, showing that fullerenes are highly stable and thus that peapods with high fullerene concentrations may prevent nanotube buckling. Note that for self-similar structures ($t/R=const$) the minimum thickness Nt required for the self-buckling is very small, thus the self-collapse is peculiar of the nanoscale and does not have a macroscopic counterpart.

2.3. Peapods

In the case of peapods, shown in Figs. 3 and 4, the collapse pressure is increased as a consequence of the presence inside the nanotube of the fullerenes; since the critical pressure of fullerenes is much higher than that of a nanotube, we treat the peapod as a nanotube of finite length L, equal to the (centre-to-centre) distance between two adjacent fullerenes. Note that the classical buckling formula of cylindrical shells assumes an infinite length for the cylinder.

According to classical elasticity [23,24], the buckling pressure for a long cylinder is:

$$p_C = \frac{3N^\alpha D}{R^3}, \quad L \gg L_c \tag{5a}$$

whereas for short cylinders [23,24] it is:

$$p_C = \frac{4\pi^2 N^\alpha D}{RL^2}, \quad L \ll L_c. \tag{5b}$$

The critical length governing the transition can be calculated equating Eqs. (5a) and (5b):

$$L_c = \frac{2\pi}{\sqrt{3}}R. \tag{6}$$

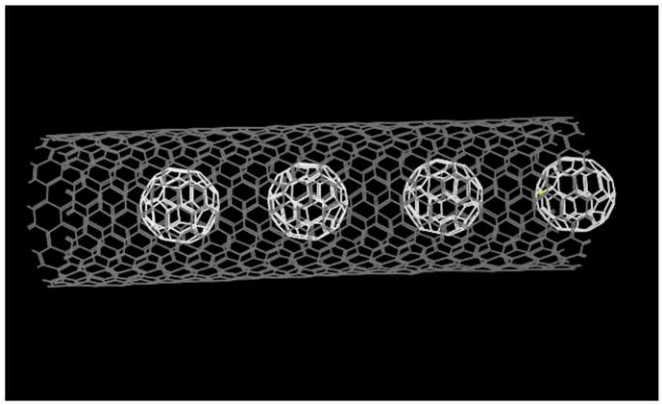

Fig. 3. Peapod treated by MD simulations.

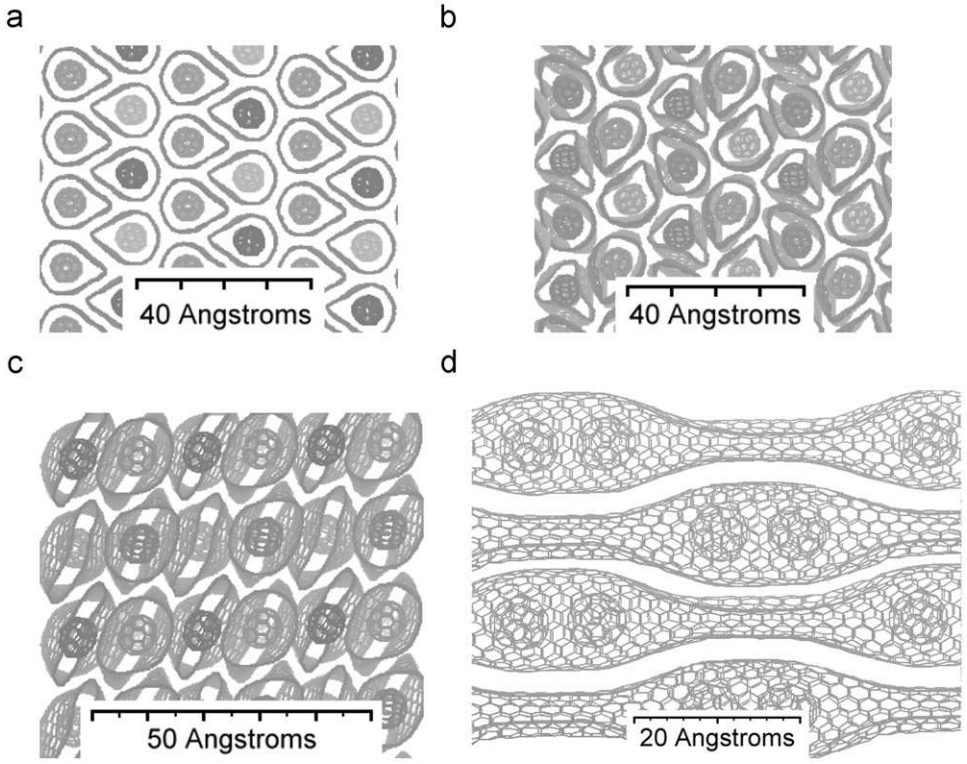

Fig. 4. Cross-section of collapsed peapods: full (a), three quarter full (b), half-full parallel to the tube axis (c), half-full perpendicular to the tube axis.

For intermediate lengths, elasticity poses [23,24]:

$$p_c = \frac{\pi^2\sqrt{\sqrt{1-\nu^2}N^\alpha D}}{RL\sqrt{Rt}}, \quad L \sim L_c. \tag{5c}$$

Revisiting the previous elastic results, we thus expect for the buckling of peapods the following regimes [12]:

$$p_C = \frac{3N^\alpha D}{R^3} - \frac{\gamma+\gamma_t}{R}, \quad L \gg L_c \tag{6a}$$

$$p_C = \frac{\pi^2\sqrt{\sqrt{1-\nu^2}N^\alpha D}}{RL\sqrt{Rt}} - \frac{\gamma+\gamma_t}{R}, \quad L \sim L_c \tag{6b}$$

$$p_C = \frac{4\pi^2 N^\alpha D}{RL^2} - \frac{\gamma+\gamma_t}{R}, \quad L \ll L_c. \tag{6c}$$

Let us introduce the fullerene content as:

$$f = \frac{2R}{L}. \tag{7}$$

Then the previous equation becomes [12]:

$$p_C = \frac{3N^\alpha D}{R^3} - \frac{\gamma+\gamma_t}{R}, \quad f \ll f_c = \frac{\sqrt{3}}{\pi} \tag{7a}$$

$$p_C = \frac{\pi^2\sqrt{\sqrt{1-\nu^2}N^\alpha D}}{2R^2\sqrt{Rt}} f - \frac{\gamma+\gamma_t}{R}, \quad f \sim f_c \tag{7b}$$

$$p_C = \frac{\pi^2 N^\alpha D}{R^3} f^2 - \frac{\gamma+\gamma_t}{R}, \quad f \gg f_c. \tag{7c}$$

These three stiffening regimes are summarised in Fig. 5.

We can estimate the ratio q between the buckling pressures for fullerene contents $f=0$ and $f=1$, as:

$$q = \frac{p_C(f=1)}{p_C(f=0)} = \frac{\pi^2 - (\gamma+\gamma_t)R^2/(N^\alpha D)}{3-(\gamma+\gamma_t)R^2/(N^\alpha D)}. \tag{8}$$

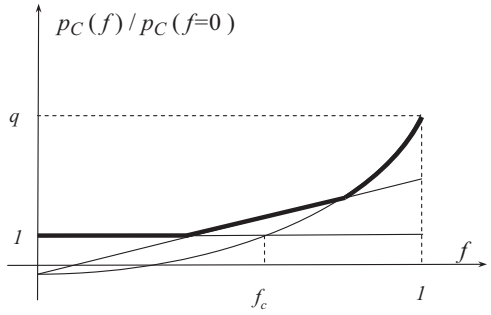

Fig. 5. Theoretical dependence of the buckling pressure vs. fullerene content: note the intermediate linear regime [12].

From Eq. (8), we expect $q > \pi^2/3$, as here confirmed by MD simulations, see Fig. 6.

From Eq. (6) we derive the following conditions for the self-buckling [12]:

$$R_C^{(N)} = \sqrt{3}\sqrt{N^\alpha}\sqrt{\frac{D}{\gamma+\gamma_t}}, \quad L \gg L_c \tag{9a}$$

$$R_C^{(N)} L_C^{(N)2} = \frac{\pi^4 D^2\sqrt{1-\nu^2}}{(\gamma+\gamma_t)^2 t}, \quad L \sim L_c \tag{9b}$$

$$L_C^{(N)} = \sqrt{2\pi}\sqrt{N^\alpha}\sqrt{\frac{D}{\gamma+\gamma_t}}, \quad L \ll L_c. \tag{9c}$$

Note that for small fullerene content the self-collapse is dictated by a critical radius, as for empty nanotubes, whereas for large fullerene content the self-collapse is dictated by a critical distance between two adjacent fullerenes (in the intermediate case, length and radius are comparable).

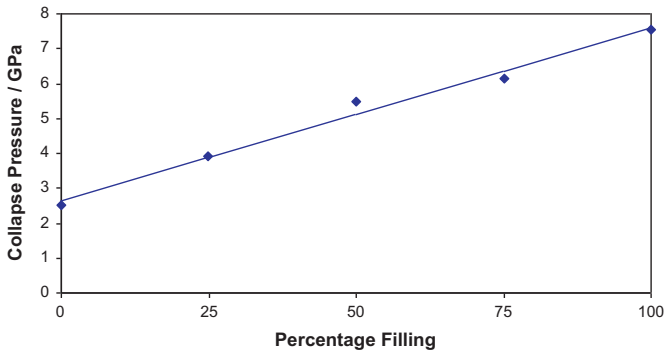

Fig. 6. Collapse pressure as a function of percentage filling computed by MD simulations (dots) vs. linear theoretical prediction (line).

3. Conclusions

New Molecular Dynamics simulations, to study the buckling and self-buckling of nanotubes, fullerenes and especially peapods, have been conducted and theoretically [12] verified; our coupled approach could have interesting applications for producing smart actuators and super-strong materials.

Acknowledgements

NMP thanks the support from the METREGEN grant.

References

[1] M.S. Dresselhaus, G. Dresselhaus, K. Sugihara, I.L. Spain, H.A. Goldberg, Graphite Fibers and Filaments, Springer-Verlag, Berlin, 1988.
[2] S. Iijima, Nature 354 (1991) 56.
[3] E.W. Wong, P.E. Sheehan, C.M. Lieber, Science 277 (1997) 1971.
[4] D.A. Walters, L.M. Ericson, M.J. Casavant, J. Liu, D.T. Colbert, K.A. Smith, R.E. Smalley, Appl. Phys. Lett. 74 (1999) 3803.
[5] M.-F. Yu, O. Lourie, M.J. Dyer, K. Moloni, T.F. Kelly, R.S. Ruoff, Science 287 (2000) 637.
[6] J. Lu, Physical Review Letters 79 (1997) 1297.
[7] B.I. Yakobson, C.J. Brabec, J. Bernholc, Physical Review Letters 76 (1996) 2511.
[8] A.Strong Kelly, Solids, Oxford University Press, Oxford, 1966.
[9] C. Lee, X. Wei, J.W. Kysar, J. Hone, Science 321 (2008) 385.
[10] R. Saito, R. Matsuo, T. Kimura, G. Dresselhaus, M. Dresselhaus, Chemical Physics Letters 348 (2001) 187.
[11] H. Staudinger, Die Hochmolekularen Organischen Verbindungen, Springer-Verlag, Berlin, 1932.
[12] N.M. Pugno, Journal of the Mechanics and Physics of Solids 58 (2010) 1397.
[13] J.A. Elliott, J.K. Sandler, A.H. Windle, R.J. Young, M.S. Shaffer, Physical Review Letters 92 (2004) 095501.
[14] M.S. Motta, A. Moisala, I.A. Kinloch, A.H. Windle, Advanced Materials 19 (2007) 3721.
[15] N. Pugno, R. Ruoff, Philosophical Magazine 84/27 (2004) 2829.
[16] N. Pugno, International Journal of Fracture 140 (2006) 159.
[17] N. Pugno, International Journal of Fracture 141 (2006) 311.
[18] N. Pugno, Applied Physics Letters 90 (2007) 043106.
[19] N.M. Pugno, Journal of Physics:Condensed Matter 18 (2006) S1971.
[20] N.M. Pugno., Acta Materialia 55 (2007) 5269.
[21] N.M. Pugno, Nano Today 2 (2007) 44.
[22] N. Pugno, Nanotechnology 17 (2006) 5480.
[23] R.M. Jones, Buckling of Bars, Plates and Shells, Bull Ridge Publishing, Blacksburg, Virginia, USA, 2006.
[24] A.V. Pogorevol, Bending of Surface and Stability of Shells, American Mathematical Society, Providence, Rhode Island, USA, 1988.